Available online at www.sciencedirect.com
ScienceDirect
Journal of Magnetic Resonance 192 (2008) 159–166
JMR Journal of Magnetic Resonance
www.elsevier.com/locate/jmr

NMR bioreactor development for live in-situ microbial functional analysis

Paul D. Majors [a,*], Jeffrey S. McLean [b], Johannes C.M. Scholten [c]

[a] *Biological Sciences Division, Pacific Northwest National Laboratory, 3335 Q Avenue, MSIN: K8-98, Richland, WA 99352, USA*
[b] *The J. Craig Venter Institute, La Jolla, CA, USA*
[c] *Merck Co. Inc., West Point, PA, USA*

Received 6 August 2007; revised 18 November 2007
Available online 16 February 2008

Abstract

A live, in-situ metabolomics capability was developed for prokaryotic cultures under controlled growth conditions. Toward this goal, a radiofrequency-transparent bioreactor was developed and integrated with a commercial wide-bore nuclear magnetic resonance (NMR) imaging spectrometer and a commercial bioreactor controller. Water suppressed ^{1}H NMR spectroscopy was used to monitor glucose and fructose utilization and byproduct excretion by *Eubacterium aggregans* (an anaerobic bacterial species relevant for biofuel production) under controlled batch and continuous culture conditions. The resulting metabolite profiles (short chain organic acids and ethanol) and trends are consistent with existing knowledge of its metabolism. However, our study also showed that *E. aggregans* produces lactate end product in significant concentrations—a result not previously reported. The advantages of live in-situ microbial metabolomics analysis and its complementariness with functional genomics/systems biology methods are discussed.

Keywords: Nuclear magnetic resonance (NMR) spectroscopy; Bioreactor; *Eubacterium aggregans*; Ethanol fermentation; In-vivo metabolomics; Bio-based products; Bioenergy

1. Introduction and background

The microbiological processing of renewable biomass (plant matter) into biofuels and other chemicals is a promising approach to reduce our dependence upon diminishing petrochemical feedstocks [1]. However, the development and optimization of bioprocessing methods requires a detailed understanding of a microbial system's metabolic pathways and flux rates. *Metabolomics* involves measuring the metabolite composition of a biological system under defined physiological conditions [2]. Nuclear magnetic resonance (NMR) spectroscopy is unique in its ability to monitor in-situ metabolic flux rates [3].

Early live, in-situ microbial metabolism NMR studies employed conventional liquid-state (test tube) NMR techniques [4,5] using washed cells with minimal environment control. Subsequent researchers developed methods to oxygenate the cell suspension while in the NMR tube [6,7] allowing for aerobic studies. Other researchers developed flow-loop systems [8,9] to transport cells from an external bioreactor to a modified NMR tube in the spectrometer. These designs suffer the loss of growth control during the long (tens of seconds) transit times, where the environment is neither regulated nor monitored. The design of Noguchi et al. [10] attempts to provide environment information by monitoring an identical flow cell in a parallel flow loop.

Several *NMR-compatible bioreactors* have been developed [11–15]. These bioreactor-in-magnet designs allow for NMR detection in or immediately adjacent to the reaction vessel, thus they provide metabolism measurements under controlled-environment conditions. Of particular note is the *membrane-cyclone* NMR bioreactor [13,16], a hydrocyclone bioreactor promoted for its simplicity of construction and operation [17]. Introduced [18] as an alternative to stirred-tank reactors operating in the sub-liter volume range,

* Corresponding author. Fax: +1 509 371 6546.
E-mail address: paul.majors@pnl.gov (P.D. Majors).

1090-7807/$ - see front matter © 2008 Elsevier Inc. All rights reserved.
doi:10.1016/j.jmr.2008.02.014

Nomenclature

Dilution rate	influent volumetric flow rate divided by the bioreactor culture volume (h^{-1})	M	molarity (mol l^{-1})
		ppm	field independent NMR chemical shift scale

hydrocyclones are ideal for NMR because they have no moving parts—a recirculation pump provides the power for both gas exchange and mixing functions. The Hartbrich reactor [13] incorporates these features plus enhanced NMR sensitivity of their earlier continuous-flow bioreactor [12]. Increased NMR sensitivity involves using reactor-suspension flow to constantly replenish the NMR test section with *fully-polarized* spins [19], thus allowing for rapid signal averaging. This allows for lower detectable metabolite concentrations and/or better temporal resolution.

Cyclones are passive vessels that—when injected with a flowing suspension—generate a centrifugal flow field to efficiently separate the suspension phases based upon their density contrast or (for solids) particle size. Cyclones consist of a cylindrical or conical vortex chamber with a tangential-flow-injection inlet and concentric outlets with characteristic geometric dimension ratios [20]. They have been employed for solid–gas [20], solid-liquid [21], liquid–liquid [22] and liquid–gas separations. Hydrocyclone *bioreactors* function as liquid–gas separators and are highly efficient due to the large density contrast [23]. Very high gas transfer rates can be obtained by introducing the influent gas as bubbles either upstream of the cyclone inlet [13] or at the chamber wall [24], leading to high cell densities and product yields [25,26].

The membrane-cyclone reactor has been applied for metabolic studies of bacterial and yeast suspensions [13,27,28]. These studies employed ^{31}P (and sometimes ^{13}C and ^{15}N) NMR methods. These nuclei readily yield adequate spectral resolution with modest effort due to their large chemical shift ranges. Further, the spectra are often less complicated than ^{1}H NMR spectra. Phosphorus is less ubiquitous in metabolites, and ^{13}C and ^{15}N measurements usually employ selectively enriched materials due to their low natural abundances (labeling of substrates allows for the selective observation of their metabolic products and largely excludes extraneous compounds). Finally, there are typically no strong solvent background signal and attendant signal suppression issues for these nuclei.

^{1}H NMR is commonly employed for NMR metabolomics studies—^{1}H is nearly 100% in natural abundance, has a high NMR sensitivity and is found in most metabolites. However, ^{1}H NMR suffers from a small chemical shift range requiring good magnetic field uniformity and somewhat longer measurement times. Additionally, the large (55 M) water signal must be attenuated by several orders of magnitude in order to detect *millimolar* metabolite signals. Further, the resulting NMR spectra reflect the metabolic complexity of the sample and require mixture-analysis post-processing [6]. This article describes the development and optimization of an NMR-transparent hydrocyclone bioreactor that is suitable for live/in-situ water-suppressed ^{1}H NMR metabolomics studies, and its application to the study of anaerobic bacterial systems relevant for bioenergy development.

2. Materials and methods

2.1. NMR bioreactor

The NMR bioreactor (Fig. 1) provides a stable, controlled growth environment for microbial suspensions during NMR measurements. It is designed to operate within a commercial widebore superconducting magnet, thus it is constructed from nonmagnetic Pyrex® glass and composite materials and has a concentric cylindrical geometry. The reactor vessel, a small sensor/sampling port manifold and a modified peristaltic pump (Fig. 1A–C) are interconnected with pump tubing (6.4 mm ID Pharmapure™, Saint-Gobain Performance Plastics, Akron, OH, USA) and supported in and atop the actively shielded 11.7 T superconducting magnet (Fig. 1D). The sensor manifold contains standard pH, temperature and dissolved oxygen sensors, plus two septum ports used for sample withdrawal and reagent injection. Materials and dimensions were designed for autoclaving and allow thermal expansion to temperatures exceeding 125 °C. The peristaltic pump employed an air-powered pump drive (Masterflex L/S model 7569-00, Cole Parmer, Vernon Hills IL USA) that was rendered compatible with the strong magnetic field by replacing its steel casing with an aluminum support platform. This recirculation system provides the power for mixing and aeration, as well NMR sensitivity enhancement [12,19].

The magnet insert is connected by an umbilical of fluid lines and sensor cables to a mobile aluminum equipment rack containing supporting equipment (not shown). This includes media and waste vessels, pumps and a commercial bioreactor controller (Fairmentec FCE 03, Bioengineering AG, Zürich CH) containing sensor and control circuitry for temperature, pH, pO_2 and redox control. A transparent, mock NMR bore tube constructed from aluminum and Lucite® tubing supports the bioreactor and allows for its safe visual inspection while operating outside of the magnet. This non-magnetic rack is rolled adjacent to the magnet and the bioreactor/pumping system is transferred into the magnet without interrupting reactor operation. Automated bioreactor control and parameter recording is obtained using InTouch data logging software (Wonderware, Lake Forest CA USA) with 1-min time resolution.

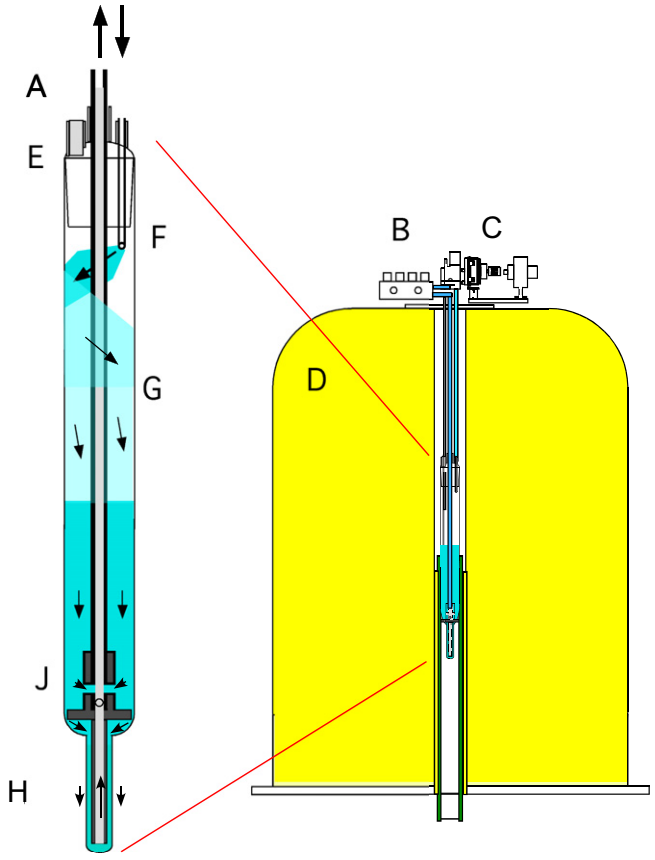

Fig. 1. Illustration of the NMR bioreactor system. A: autoclavable Pyrex bioreactor vessel (scale 4:1); B: sensor manifold, C: recirculation pump; D: actively shielded widebore superconducting magnet; E: vessel lid; F: tangential flow injector; G: reaction chamber; H: NMR test section; J: Ultem™ tube extender with bubble-deflection plate and flow bypass gate. The arrows indicate the flow paths for the suspended culture.

The vessel lid (Fig. 1E) employs a 55/50 standard taper ground glass joint. It contains four ports: a 7 mm ID internally threaded glass connector with an O-ring seal as a feedthrough for the 5 mm OD tangential fluid injector line; a concentric 11 mm ID connector for the 10 mm OD return line; a second 11 mm ID connector to support multiple fluid lines (acid, base, gas and media influent lines and media effluent line to maintain a safe fluid level); and a hose barb for 12 mm tubing connected to a vapor condensation tube (not shown) serves as the gas outlet. The bottom, fluid-fed 20 mm OD cylindrical test section (Fig. 1H) effectively replaces a conventional NMR sample tube.

The in-magnet bioreactor vessel (Fig. 1A) is modeled closely after the membrane-cyclone reactor [13]. The microbial suspension is tangentially injected into the cylindrical reaction chamber (Fig. 1F), which provides mixing and the efficient removal of entrained gas by centrifugal force. Gas exchange is accomplished by purging the reaction vessel with influent gas, which exchanges with the media gases via the expanded falling film surface area on the reaction vessel wall. [Purging the vessel with N_2 gas at a low flowrate was experimentally determined to yield strict anaerobic growth conditions in less than 1 h.] The flow from the mixing chamber to the test section is partially restricted by a impermeable plate (Fig. 1J) with a 2.5 mm clearance at the vessel wall to exclude gas bubbles. An adjustable flow inlet above the plate allows for the partial bypassing of the test section, thus decoupling the test section replenishment (NMR optimization) flow rate from the overall flow (mixing) rate [16]. The suspension flows into the test tube section (Fig. 1H) where NMR measurements are performed. A concentric, internal *return tube* lifts the suspension from the test section to the sensor manifold and pump, and is injected into the mixing chamber to complete the circulation loop.

The reactor was optimized for ^{1}H NMR spectroscopy by: (1) integrating it with magnetic field gradient hardware to allow gradient-assisted water suppression and other NMR experiments employing gradients, (2) reducing the flow rate at the test section to increase the mean fluid-residence time to approximately one second to accommodate a longer NMR signal detection interval, and (3) reconfiguring the test section (geometry and materials) to yield a spectral line width adequate for water suppression. A spreadsheet program was developed and used to optimize the hydro-cyclone reaction vessel and to determine safe operating conditions. The program input includes fluid properties (dynamic viscosity and density), NMR properties (longest anticipated T_1 and T_2 spin relaxation times) and reactor parameters (test section, reaction chamber and tubing dimensions). Program output includes the optimum flow rates (0.6–1.2 liter/min constant flowrate) and corresponding Hagen–Poiseuille pressures, and the minimum required reaction volume for optimal NMR sensitivity [12].

2.2. Cultivation experiments

Batch and continuous cultivation experiments with bacterium *Eubacterium aggregans* were performed with a bioreactor culture volume of 200 ml at 33 °C and the pH was maintained at 7 by base (0.05 M NaOH) addition during all experiments. Prior to inoculation with *E. aggregans* (20% by volume), the NMR bioreactor with medium was adjusted to the desired growth conditions (anaerobic, pH 7, $T = 33$ °C) and baseline NMR measurements were performed. Subsequently, an anaerobic inoculum of bacteria (prepared and stored under an atmosphere of mixed 95% N_2 and 5% CO_2) was introduced via the influent line. Measurement runs consisted of a controlled-batch incubation with glucose (40 mM) followed by a continuous cultivation experiment with the same sample. The dilution rate was set at 0.14 h^{-1} with no cell retention for the continuous cultivation experiments, and *E. aggregans* was grown with influent media containing different concentrations of glucose (5, 40 and 20 mM) and finally fructose (20 mM; relative starting times $t = 0$, 20, 27 and 50 h, respectively) as the growth-limiting substrates. *E. aggregans* (DSM

12183) was purchased from the Deutsche Sammlung von Mikroorganismen und Zellkulturen (Braunschweig, Germany) and grown in bicarbonate-buffered, sulfide-reduced mineral medium as described previously [29].

A separate fed-batch cultivation experiment with a high-biomass-density of *E. aggregans* was performed in the NMR bioreactor at 33 °C. The residence times of medium and cells were decoupled by a circulation-integrated cross-flow hollow fiber module (0.1 micron pore Xampler™, GE Healthcare, Piscataway, NJ, USA) inserted between the pump and vessel inlet to achieve higher cell densities as compared to continuous fermentations without cell retention. The working volume of the NMR bioreactor was 200 ml and the pH was not controlled. Medium adjustments and baseline NMR measurements were performed as described above. An anaerobic inoculum of bacteria (prepared and stored under an atmosphere of mixed 95% N_2 and 5% CO_2) was subsequently introduced via the influent line. The measurement run consisted of batch incubation with glucose (20 mM) obtained by injecting 4 ml 1 M glucose into the septum port. The cells were retained in the bioreactor and the final cell-density was 1.5 g dry weight per liter.

2.3. NMR studies

All NMR measurements were performed using a Bruker Avance imaging spectrometer with a 11.7 T superconducting magnet with a 89 mm diameter accessible bore operating at a Larmor frequency of 500.14 MHz for hydrogen-1. NMR imaging hardware included a Bruker Mini0.5 XYZ gradient probe (35 G/cm gradients) driven by 60-ampere Bruker gradient amplifiers. Radiofrequency (RF) excitation and detection were accomplished using a Bruker Mini0.5 RF insert containing a 38 mm ID birdcage detection coil and tuned for 500 MHz. The bioreactor was carefully centered within the imaging gradients by performing multidirectional NMR imaging (MRI) of the test section. The magnetic field uniformity over the test section was corrected using all first and second order terms by implementing the FASTMAP [30] automated shimming procedure with no recirculation flow.

Water-suppressed ^{1}H NMR spectra were acquired using the improved WATERGATE pulse sequence (W5 version, Bruker pulse program zggpw5.ppg) [31]. This sequence provides good phase uniformity, a wide inversion (spectral) bandwidth and narrow solvent-suppression bandwidth to allow detection of resonances close to that for water. Consecutive water-suppressed ^{1}H NMR spectra were acquired with 64-560 1.07-s repetitions for a time resolution of 1.1–10 min. A 0.5 s delay was followed by the WATERGATE W5 pulse train with 400-μs interpulse spacings resulting in an inversion bandwidth of ~5000 Hz. The duration for rectangular RF pulses with 90-deg nutation angles was 68 μs. Water suppression employed two sets of 1-ms half-sine gradient pulses (two bipolar pairs with 4.8 and 3.4 G/cm maximum amplitudes) applied in the *Y* direction, i.e. tangential to fluid flow (*Z* direction) to minimize velocity-induced signal losses. The resulting NMR echo signal was sampled with 4096 complex points over an acquisition interval 0.511 seconds, yielding a spectral bandwidth of 8013 Hz. (Data were acquired without active magnetic field (lock) stabilization—this was deemed acceptable as the exceptionally stable magnet system generally shows negligible field drift over the period of weeks.) WATERGATE W5 resulted in a water suppression factor of approximately 300. NMR data were processed using TopSpin (v. 1.3, Bruker Instruments) NMR application software, by applying 5 Hz of Lorentzian line broadening, Fourier transformation, and first order phase correction. Baseline correction was performed by applying a cubic spline fit to selected baseline points. This procedure was automated using a serial processing script. Chemical shifts were referenced by (a) measuring the non-suppressed water signal and assigning its temperature-dependent shift value [32], then (b) internally by setting the lactate CH_3 spectral line to its known value of 1.33 ppm.

The processed spectral data were next integrated using a predefined integration range file. The integration regions included the formate, lactate (CH and CH_3), sugar, *n*-butyrate (C2 and C3 CH_2 peaks and CH_3 peak), pyruvate, acetate and ethanol CH_3 peaks. A TopSpin automation program was used to accumulate the experiment number, acquisition date and time, number of scans, receiver gain, and numerical integration value for each region into a comma-separated-value (CSV) text file for import into a spreadsheet program. The spectral integration values were imported into Excel spreadsheet program (Microsoft Corp., Redmond, WA, USA). The peak areas were subsequently quantified and calibrated to yield molar concentrations for the respective metabolites by: (1) correcting for intensity variation with offset frequency (determined in a separate WATERGATE experiment by measuring the media water-line intensity while changing the carrier frequency); (2) normalizing receiver gain and number of repetitions; and (3) correcting for spin count (additionally, supervised deconvolution of overlapping spectral lines was implemented as needed to resolve overlapping lactate and ethanol resonances, and to separate overlapping glucose-and-fructose and glucose-and-ethanol lines). Finally, the time-resolved NMR data were synchronized and integrated with the bioreactor environment log data.

The processed time series spectra were later subjected to unsupervised principle component analysis (PCA; Amix v 3.5 software; Bruker Instruments) to provide an unbiased identification of significant i.e. responsive metabolites. One hundred twenty-two spectra were descretized (*bucketed*) into 0.05 ppm increments (8.6–8.4 ppm and 4.3–0.6 ppm which excluded the remaining water resonance).

3. Results

Batch and continuous cultivation experiments with *E. aggregans* were conducted to assess NMR-bioreactor per-

formance. These experiments (Figs. 2 and 3) yielded the time-resolved consumption of substrate (glucose or fructose) and the identities and concentrations of the resulting end products. The observed end products were lactate, acetate, formate, *n*-butyrate, ethanol and pyruvate and are summarized in Table 1 (the spectral-line assignment of pyruvate is tentative and may instead correspond with succinate. Further experiments are required to positively identify this line). These products are all extracellular–intracellular metabolites were not detected due to the low cell densities and modest spectral resolution employed in these studies.

Fig. 2 shows the resulting time-resolved concentrations for the detected glucose and end-products during the batch run. Glucose decreased from 40 to 1.3 mM after 23 h. Concurrently, the organic acid products were seen to increase in an approximately linear fashion, with lactate four times more abundant than formate or acetate (Fig. 2). The consumption of glucose revealed a undetected ethanol resonance—unsupervised PCA analysis clearly resolved the ethanol CH_2 resonance at 3.65 ppm, which was buried under the glucose resonances during much of the run, and led to the identification of a shoulder of the lactate peak (approx. 1.2 ppm) as the CH_3 resonance of ethanol.

Fig. 3 shows time-resolved substrate and end-product concentrations for a continuous 3-day NMR bioreactor run using *E. aggregans*. This study immediately followed the batch glucose-utilization study (Fig. 2). During Run_1 ($t = 0$–20 h) 5 mM glucose was applied with a dilution rate of 0.14 h^{-1}. After 11.8 h, the glucose was consumed and lactate decreased to sub-millimolar values, clearly revealing both ethanol resonances. The remaining organic acid products remained at moderately high levels, with acetate the highest at 2–2.5 mM. During Run_2 ($t = 20$–50 h) the glucose concentration was changed to 40 mM, then 20 mM glucose leading to an overall increase in lactate, butyrate, and ethanol and a decrease in formate and pyruvate, with acetate remaining fairly constant. Finally in Run_3 ($t = 50$–76 h) the substrate was switched to 20 mM fructose at a dilution rate of 0.14 h^{-1}, yielding a slowly increasing lactate and/or ethanol concentration, while the other products remained constant and unchanged from the immediately preceding glucose run. After switching substrates in the influent feed, the glucose concentration decreased to an undetectable level after approximately 4 h, and fructose increased to a maximum value of 7.7 mM after approximately 8 h.

The high-biomass fed-batch cultivation experiment resulted in the consumption of all glucose after 30.7 h and production of similar end products as observed in the previous batch and continuous cultivation experiments. However all products were at or below 7 mM and the lactate concentration began steadily decreasing after the glu-

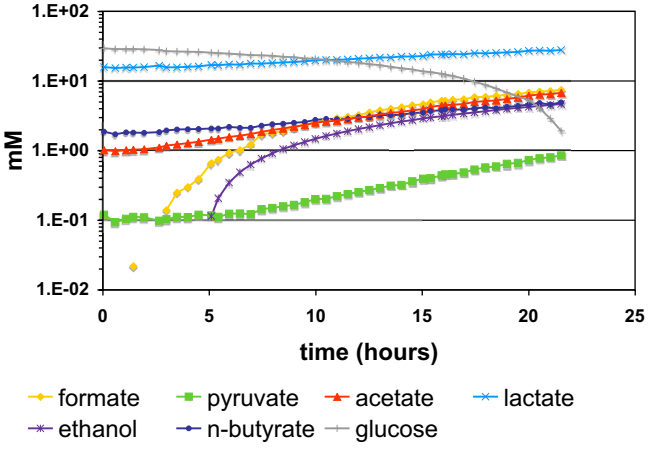

Fig. 2. Semilogarithmic plot of metabolite concentrations versus reaction time derived from water suppressed time-series ^{1}H NMR data for a *E. aggregans batch* glucose utilization study. Approximately every sixth time point is shown (1-h increments).

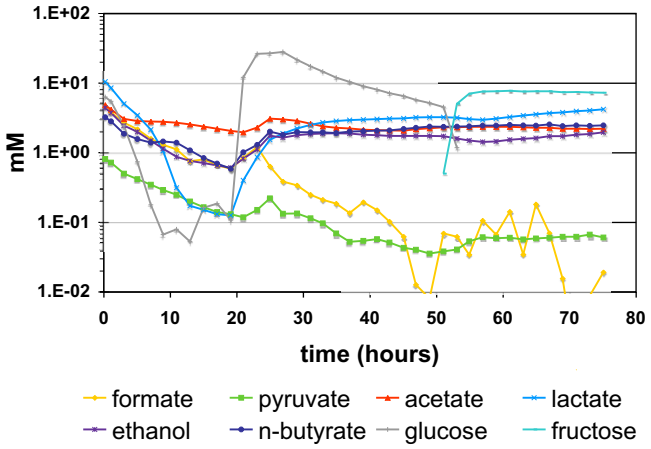

Fig. 3. Semilogarithmic plot of metabolite concentrations versus reaction time derived from water suppressed time-series ^{1}H NMR data for a *E. aggregans chemostat* glucose-then-fructose utilization study. Approximately every twelfth time point is shown (2-h increments).

Table 1
Experimental end-product yield values for *E. aggregans* grown on glucose or fructose during batch and continuous cultivation

End-product	Ratio mol_P[a]/mol_S[b]			
	Batch[c]	Run 1[d]	Run 2[e]	Run 3[f]
Formate	0.28	0.17	0	0
Pyruvate	0.03	0.03	0	0
Acetate	0.22	0.45	0.15	0.18
Lactate	0.46	0	0.26	0.35
Ethanol	0.17	0.22	0.09	0.09
n-Butyrate	0.12	0.15	0.16	0.20

[a] P: product.
[b] S: substrate.
[c] Determined for end of batch run $t = 21.4$ h (Fig. 2).
[d] Determined near end of first continuous run ($t = 16.9$ h; 5 mM glucose starting concentration; final glucose concentration below detection levels at $t = 11.8$ h; Fig. 3).
[e] Determined near end of second continuous run ($t = 47.3$ h; 20 mM glucose starting concentration; 5.6 mM final glucose concentration).
[f] Determined near middle of third continuous run ($t = 67.7$ h; 20 mM fructose starting concentration; 7.5 mM final fructose concentration).

cose supply was exhausted (data not shown). Formate was not detected at any time.

4. Discussion

The measured end product yields (mol_product mol_substrate^{-1}) for the different runs are given in Table 1. Glucose was consumed completely during the batch incubation (Fig. 2). During the chemostat glucose and fructose utilization study residual carbohydrate concentrations remained in the bioreactor (Fig. 3). The fructose concentration attained only 38% of the feed concentration, as it was introduced at a moderate dilution rate into an actively-metabolizing cell suspension, demonstrating the rapid adaptation of the *E. aggregans* culture to the new substrate. These trends are predicted based on the steady-state relationship between the concentration of substrate in the in-flowing medium and the dilution rate. The end products changed only slightly with the change of substrate from glucose to fructose. *E. aggregans* is known to ferment carbohydrates like glucose and fructose to produce end-products like formate and butyrate (glucose), and acetate and butyrate (fructose), respectively. However, our study showed that lactate is a very important end-product (Table 1) something that was overlooked in a previous study [33]. Having meaningful data on the amount of substrate utilized and end-product produced allowed us to construct a macro-chemical equation [34] for the fermentation of both sugars (data not shown). Our calculations also show that the end-products for both glucose and fructose are very similar in agreement with experimental Run 3 (Table 1). The calculations also indicate that other fermentation end-products like dihydrogen (H_2) and carbon dioxide must have been formed; however, these products were not measured with the NMR technology. Combining liquid-state NMR with gas-phase mass spectrometry (MS) of the reactor effluent gas would yield all of the important stoichiometric coefficients for the characterization of biomass fermentation and enable the determination of maximum efficiency for its conversion to biofuels.

The high-biomass study resulted in lower proportional yields than the previous cultivation experiments. Our calculations [29] showed that the sum of fermentation products by accounting for the elements C, H and O was too low to explain the glucose consumption for the high-biomass study. This might be explained by a shift to the production of end products that were not detectable by NMR. The NMR spectral resolution for the high-biomass study was degraded in comparison with the previous studies—intermittent MRI measurements (not shown) showed the presence of transitory biomass deposits in the test section were a likely cause of the spectral broadening. Thus, further optimization is required to perform adequate high-

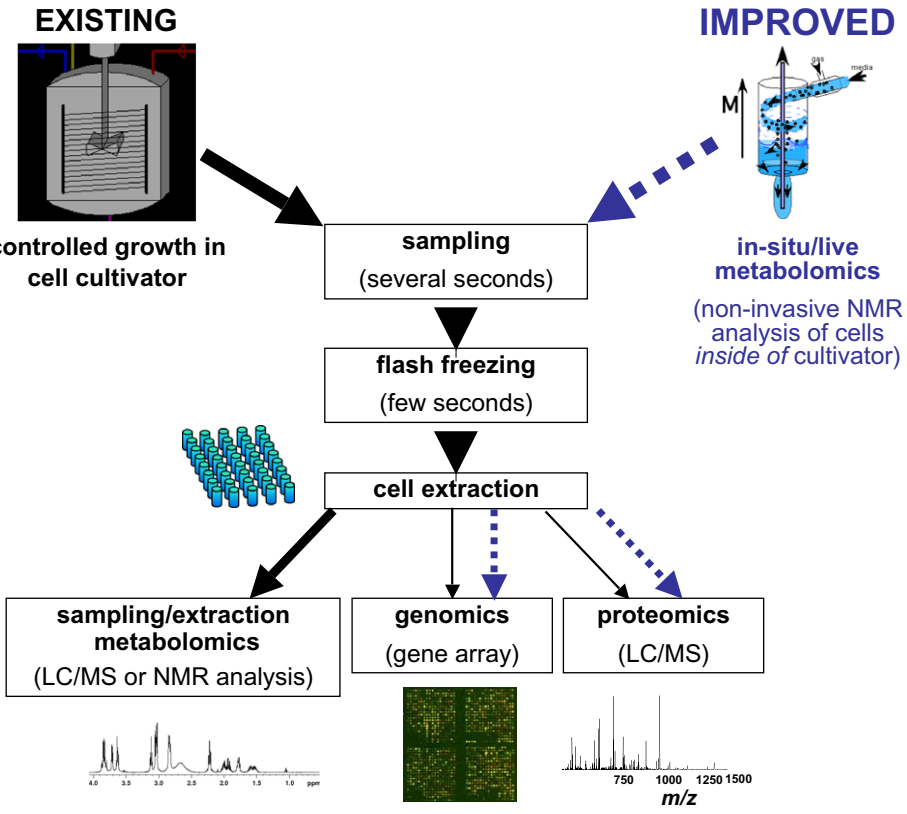

Fig. 4. Flowchart comparing *existing* (solid arrows) and *live* in-situ (dashed arrows) metabolomics paradigms. The sampling/freezing steps of existing methods consume material and can distort metabolite profiles. The live in-situ method uses NMR to collect metabolomics data while inside of the controlled bioreactor, saving the entire sample for genomics and proteomics.

biomass studies. Although an internal concentration reference was not employed, the external water signal and internal *n*-butyrate and pyruvate signals gave consistent intensities thus the low product concentrations are deemed accurate.

Existing systems biology techniques which seek to combine metabolomic with transcriptomic and proteomic data (Fig. 4; solid black arrow path) involve *sampling* live cells from a bioreactor, rapidly halting their metabolism (*freezing*), then chemically *extracting* the metabolite contents for detection by NMR, MS, gas chromatography, capillary electrophoresis or high-performance liquid chromatography analysis. Since metabolite profiles change on a *second to sub-second timescale* [35,36], these profiles can be *corrupted* during the several seconds required for sampling and freezing. (Protein, DNA and RNA profiles change on timescales of minutes to hours [37,38] and are more robust to sampling.) Attempts have been made to minimize sampling/freezing distortions [39,40]. Finally, the reaction culture contents are incrementally diminished or diluted with each sampling, resulting in poor efficiency.

Another approach is to draw upon the non-invasive nature of NMR to measure metabolism while inside of a functioning bioreactor (Fig. 4; top right). In this *systems biology paradigm*, metabolic data are collected *prior to* genomics/proteomics. The advantages include: (1) accurate metabolite concentrations and profiles acquired under rigorously controlled dynamic or steady-state growth conditions; (2) non-destructive measurements that preserve the entire sample volume for genomics and proteomics (Fig. 4; dashed arrows); (3) improved efficiency via flow-enhancement of NMR sensitivity; (4) ample time for long-duration, high-information multi-dimensional NMR measurements and stable isotope-labeling studies (since cell cultivation typically requires days or weeks of time); (5) metabolomics data can be reliably associated with subsequent genomic and proteomic measurements, since mRNA and proteins are less susceptible to sampling artifacts; and (6) prior in-situ metabolite data could be used to optimize the sampling time for genomics/proteomics/enzyme-activity analysis, e.g., after a perturbation such as the addition of a different feed stock during an ethanol fermentation study.

The current NMR bioreactor provides moderate-to-poor spectral resolution—apparently the large 20 mm outer diameter NMR test section is too large for magnetic field correction using the existing room temperature shim set. Improved spectral resolution and better water suppression are likely attainable by employing a 10 mm test tube. Figs. 2 and 3 indicate a detectable spin-concentration threshold of 0.1 mM, which will likely improve with better resolution and a NMR probe with a better filling factor. More recently, we tested a electric motor recirculation pump—the resulting flow was less pulsatile and this reduced the scan-to-scan variability allowing for the reproducible measurement of metabolite concentrations in seconds. Further optimization is needed to adequately perform high-biomass-density studies.

Acknowledgments

The researchers gratefully acknowledge Mr. Jay Draper (Northwest Technical Glass, Richland, WA) and Mr. Mark Townsend and coworkers in the EMSL Machine Shop for advice and for the construction of the NMR bioreactor components. We also acknowledge Prof. John Sheppard (Food Science Dept., North Carolina State University) for early hydro-cyclone bioreactor discussions. We also thank the Microbial Cell Dynamics Laboratory (MCDL) at PNNL for use of the controlled cultivation technologies applied in this research. This research was supported by the Laboratory Directed Research and Development Program at the Pacific Northwest National Laboratory, a multiprogram national laboratory operated by Battelle for the U.S. Department of Energy under Contract DE-AC05-76RL01830. The research was performed in the Environmental Molecular Sciences Laboratory (a national scientific user facility sponsored by the Department of Energy's Office of Biological and Environmental Research) located at Pacific Northwest National Laboratory and operated for DOE by Battelle.

References

[1] L.A. Lucia, D.S. Argyropoulos, L. Adamopoulos, A.R. Gaspar, Chemicals and energy from biomass, Can. J. Chem. 84 (2006) 960–970.
[2] J.P. Grivet, A.M. Delort, J.C. Portais, NMR and microbiology: from physiology to metabolomics, Biochimie 85 (2003) 823–840.
[3] K. Schugerl, Progress in monitoring, modeling and control of bioprocesses during the last 20 years, J. Biotechnol. 85 (2001) 149–173.
[4] T. Ogino, Y. Arata, S. Fujiwara, Proton correlation nuclear magnetic resonance study of metabolic regulations and pyruvate transport in anaerobic *Escherichia coli* cells, Biochemistry 19 (1980) 3684–3691.
[5] K.Y. Alam, D.P. Clark, Anaerobic fermentation balance of *Escherichia coli* as observed by in vivo nuclear magnetic resonance spectroscopy, J. Bacteriol. 171 (1989) 6213–6217.
[6] L. Brecker, D.W. Ribbons, Biotransformations monitored in situ by proton nuclear magnetic resonance spectroscopy, Trends Biotechnol. 18 (2000) 197–202.
[7] C. Lambert, D. Weuster-Botz, R. Weichenhain, E.W. Kreutz, A.A. De Graaf, S.M. Schoberth, Monitoring of inorganic polyphosphate dynamics in Corynebacterium glutamicum using a novel oxygen sparger for real time P-31 in vivo NMR, Acta Biotechnol. 22 (2002) 245–260.
[8] R.Z. Chen, J.E. Bailey, Observations of aerobic, growing *Escherichia coli* metabolism using an online nuclear magnetic resonance spectroscopy system, Biotechnol. Bioeng. 42 (1993) 215–221.
[9] A.R. Neves, A. Ramos, M.C. Nunes, M. Kleerebezem, J. Hugenholtz, W.M. de Vos, J. Almeida, H. Santos, In vivo nuclear magnetic resonance studies of glycolytic kinetics in *Lactococcus lactis*, Biotechnol. Bioeng. 64 (1999) 200–212.
[10] Y. Noguchi, N. Shimba, H. Toyosaki, K. Ebisawa, Y. Kawahara, E. Suzuki, S. Sugimoto, In vivo NMR system for evaluating oxygen-dependent metabolic status in microbial culture, J. Microbiol. Methods 51 (2002) 73–82.
[11] C.D. Castro, A.P. Koretsky, M.M. Domach, Performance trade-offs in in situ chemostat NMR, Biotechnol. Prog. 15 (1999) 185–195.
[12] A.A. Degraaf, R.M. Wittig, U. Probst, J. Strohhaecker, S.M. Schoberth, H. Sahm, Continuous-flow NMR bioreactor for invivo studies of microbial cell suspensions with low biomass concentrations, J. Magn. Reson. 98 (1992) 654–659.

[13] A. Hartbrich, G. Schmitz, D. WeusterBotz, A.A. deGraaf, C. Wandrey, Development and application of a membrane cyclone reactor for in vivo NMR spectroscopy with high microbial cell densities, Biotechnol. Bioeng. 51 (1996) 624–635.
[14] A.J. Meehan, C.J. Eskey, A.P. Koretsky, M.M. Domach, Cultivator for NMR studies of suspended cell cultures, Biotechnol. Bioeng. 40 (1992) 1359–1366.
[15] B.K. Melvin, J.V. Shanks, Influence of aeration on cytoplasmic pH of yeast in an NMR airlift bioreactor, Biotechnol. Prog. 12 (1996) 257–265.
[16] D. Weuster-Botz, A. de Graaf, Reaction engineering methods to study intracellular metabolite concentrations, Adv. Biochem. Eng. Biotechnol. 54 (1996) 75–108.
[17] P.S.S. Dawson, Cyclone column fermentor, Biotechnol. Bioeng. (1973) 809–819.
[18] P.S.S. Dawson, A Continuous-flow culture apparatus: The cyclone column unit, Can. J. Microbiol. 9 (1963) 671–687.
[19] G. Suryan, Nuclear resonance in flowing liquids, Proc. Indian Acad. Sci. A33 (1951) 107–111.
[20] A.K. Coker, Understand cyclone design, Chem. Eng. Prog. 89 (1993) 51–55.
[21] L.M. Tavares, L.L.G. Souza, J.R.B. Lima, M.V. Possa, Modeling classification in small-diameter hydrocyclones under variable rheological conditions, Miner. Eng. 15 (2002) 613–622.
[22] M.V. Melo, G.L. Sant'Anna, G. Massarani, Flotation techniques for oily water treatment, Environ. Technol. 24 (2003) 867–876.
[23] L. Grady, G.T. Daigger, H.C. Lim, Biological Wastewater Treatment, Marcel Dekker, New York, 1999.
[24] D. Thoenes, Chemical Reactor Development, Springer, New York, 1994.
[25] J.D. Sheppard, P. Marchessault, T. Whalen, Production of poly-beta-hydroxybutyrate in a cyclone bioreactor, Trans. ASAE 37 (1994) 521–526.
[26] D. Riesenberg, R. Guthke, High-cell-density cultivation of microorganisms, Appl. Microbiol. Biotechnol. 51 (1999) 422–430.
[27] M. Tesch, A.A. de Graaf, H. Sahm, In vivo fluxes in the ammonium-assimilatory pathways in *Corynebacterium glutaunicum* studied by N-15 nuclear magnetic resonance, Appl. Environ. Microbiol. 65 (1999) 1099–1109.
[28] B. Gonzalez, A. de Graaf, M. Renaud, H. Sahm, Dynamic in vivo P-31 nuclear magnetic resonance study of *Saccharomyces cerevisiae* in glucose-limited chemostat culture during the aerobic–anaerobic shift, Yeast 16 (2000) 483–497.
[29] J.C.M. Scholten, R. Conrad, Energetics of syntrophic propionate oxidation in defined batch and chemostat cocultures, Appl. Environ. Microbiol. 66 (2000) 2934–2942.
[30] R. Gruetter, Automatic, localized invivo adjustment of all 1st-order and 2nd-order shim coils, Magn. Reson. Med. 29 (1993) 804–811.
[31] M.L. Liu, X.A. Mao, C.H. Ye, H. Huang, J.K. Nicholson, J.C. Lindon, Improved WATERGATE pulse sequences for solvent suppression in NMR spectroscopy, J. Magn. Reson. 132 (1998) 125–129.
[32] J.C. Hindman, Proton resonance shift of water in gas and liquid states, J. Chem. Phys. 44 (1966) 4582–4592.
[33] T. Mechichi, M. Labat, T.H.S. Woo, P. Thomas, J.L. Garcia, B.K.C. Patel, *Eubacterium aggregans* sp nov., a new homoacetogenic bacterium from olive mill wastewater treatment digestor, Anaerobe 4 (1998) 283–291.
[34] J.J. Heijnen, J.P. Vandijken, In search of a thermodynamic description of biomass yields for the chemotrophic growth of microorganisms, Biotechnol. Bioeng. 39 (1992) 833–858.
[35] W. Dekoning, K. Vandam, A method for the determination of changes of glycolytic metabolites in yeast on a subsecond time scale using extraction at neutral pH, Anal. Biochem. 204 (1992) 118–123.
[36] U. Theobald, W. Mailinger, M. Baltes, M. Rizzi, M. Reuss, In vivo analysis of metabolic dynamics in *Saccharomyces cerevisiae*. 1. Experimental observations, Biotechnol. Bioeng. 55 (1997) 305–316.
[37] D. Nercessian, R.D. Conde, Control of ribosome turnover during growth of the haloalkaliphilic archaeon *Natronococcus occultus*, Res. Microbiol. 157 (2006) 625–628.
[38] A. Belle, A. Tanay, L. Bitincka, R. Shamir, E.K. O'Shea, Quantification of protein half-lives in the budding yeast proteome, Proc. Natl. Acad. Sci. USA 103 (2006) 13004–13009.
[39] S. Buziol, I. Bashir, A. Baumeister, W. Claa?en, N. Noisommit-Rizzi, W. Mailinger, M. Reuss, New bioreactor-coupled rapid stopped-flow sampling technique for measurements of metabolite dynamics on a subsecond time scale, Biotechnol. Bioeng. 80 (2002) 632–636.
[40] J. Schaub, C. Schiesling, M. Reuss, M. Dauner, Integrated sampling procedure for metabolome analysis, Biotechnol. Prog. 22 (2006) 1434–1442.